Palladium Nanoparticle Enhanced Giant Photoresponse at $LaAlO_3$/$SrTiO_3$ Two-Dimensional Electron Gas Heterostructures

Ngai Yui Chan,[†] Meng Zhao,[†] Ning Wang,[†] Kit Au,[†] Juan Wang,[†] Lai Wa Helen Chan,[†] and Jiyan Dai[†,‡,*]

[†]Department of Applied Physics, The Hong Kong Polytechnic University, Hung Hom, Kowloon, Hong Kong, People's Republic of China and [‡]Shenzhen Research Institute, The Hong Kong Polytechnic University, People's Republic of China. N.Y. and J.Y. conceived and designed the experiments. N.Y., Z.M., and W.N. performed the experiments. W.J. performed the TEM characterization. N.Y. analyzed the data together with K.A., H.L.W., and J.Y. All authors discussed the results and commented on the manuscript.

ABSTRACT With $LaAlO_3$ surface modification by Pd nanoparticles, $LaAlO_3/SrTiO_3$ (LAO/STO) interfacial two-dimensional electron gas presents a giant optical switching effect with a photoconductivity on/off ratio as high as 750% under UV light irradiation. Pd nanoparticles with a size around 2 nm are deposited on top of the LAO surface, and the LAO/STO interface exhibits a giant response to UV light with a wavelength shorter than 400 nm. This giant optical switching behavior has been explained by the Pd nanoparticle's catalytic effect and surface/interface charge coupling.

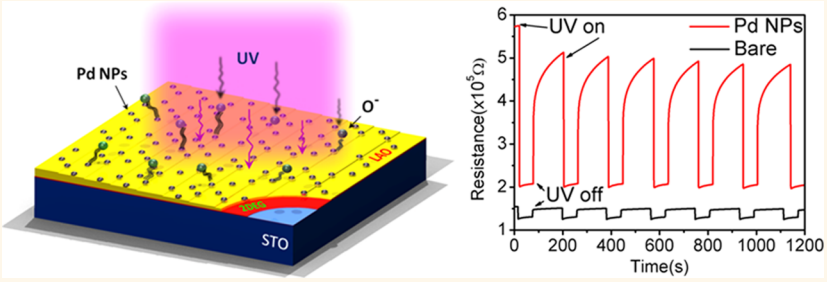

KEYWORDS: $LaAlO_3/SrTiO_3$ · interface · two-dimensional electron gas · photoresponse

Recent studies showed that a polar oxide heterostructure with conducting states can be generated at the interfaces between two large band gap insulators, and unexpected physical properties have been observed in such structures.[1] The discovery of the two-dimensional electron gas (2DEG) at the interface between two band insulators, $LaAlO_3$ (LAO, E_g = 5.6 eV) and $SrTiO_3$ (STO, E_g = 3.2 eV),[2] has triggered intensive study on this system. Intriguing electronic properties[3−5] have been found for this heterointerface, and the significant results promise potential applications in the new generation of electronic devices.[6−8]

The conduction mechanism of the oxide 2DEG has been attributed to the intrinsic polar catastrophe scenario,[2] where the polar LAO films grown on a nonpolar TiO_2-terminated STO substrate induce a charge transfer from the LAO layer to the interface by the built-in electric field in the LAO layer. However, the presence of the internal electric field in the LAO layer was doubted by the X-ray photoemission measurement result.[9,10] Some of the reports argued that the intermixing of cations around the interface[11,12] and doping of STO by oxygen vacancies[13,14] during the thin film deposition may also contribute to the 2DEG formation. A recent paper has reported an experimental study of the correlation between the interface and the surface states, and it has been suggested that the modulation of the surface state by polar liquid on the LAO/STO surface has a great influence on the transport properties of the interface.[15] We also demonstrated that the transport properties of the interfacial conducting states are extremely sensitive to the surface "polar" absorbates, and the conducting state of the interface may change to semiconducting due to the induced polar field.[16]

More recently, several groups have demonstrated that the photoconductivity of LAO/STO[17,18] and NGO/STO[19] arose from the pure "interface" effect. This brings up considerable interest in using the oxide interface 2DEG in the development of optoelectronic applications such as an optical switching

* Address correspondence to jiyan.dai@polyu.edu.hk.

Received for review June 10, 2013 and accepted September 4, 2013.

Published online September 04, 2013
10.1021/nn4029184

© 2013 American Chemical Society

device[20] or photodetector.[21] However, the photoconductivity effect in such systems is not large enough toward real application by noticing that the "states" of the LAO/STO surface affect the transport properties strongly and the fact that the presence of metallic overlayers or surface defects (oxygen vacancies) on the LAO/STO surface alters the band alignment and electronic properties of the interface.[22,23] In this report, we propose to use metal nanoparticles to modify the transport properties and improve the photoconductivity effect. We demonstrate that the Pd nanoparticle (NP)-coated LAO/STO heterostructure exhibits a giant photoresponse in the UV range. The reason to select Pd is that Pd NPs play an important role in many enhanced light sensing and gas sensing applications as a catalytic material in different kinds of metal oxide systems (*e.g.*, ZnO,[24] SnO_2,[25] and TiO_2[26]), as they provide "electroactive sites" and excellent oxidation capability on the surface to modify the transport properties of the oxides.

$LaAlO_3$ thin films with 5 u.c. (unit cell) thickness were deposited on TiO_2-terminated STO (001) substrates, where the growth conditions were the same as those reported elsewhere.[16] After the deposition, Pd NPs were deposited on top of the surface of the LAO/STO heterostructure by means of dc magnetron sputtering at room temperature. This room-temperature-grown Pd NP layer has very weak adhesion and can be removed easily by surface cleaning using cotton tips with methanol; thus, there should not be epitaxial growth on the LAO layer. Control samples (LAO/STO) without Pd NP deposition were also fabricated as a reference. Pd NPs were also deposited on TiO_2-site-terminated STO substrate (without LAO), showing that the Pd NPs are well below the conduction percolation threshold and no photoconductivity effect is observed.

RESULTS

Figure 1(a) is an AFM image showing the surface morphology of the Pd NP-coated LAO/STO sample. The disappearance of the surface terrace suggests the coverage of the LAO surface by Pd NPs. (Figure S1 shows the surface morphology of the bare TiO_2-terminated STO substrate and LAO/STO surface by AFM, where a clear terrace can be observed.) In order to confirm the existence of Pd NPs on the LAO surface and to know their structural characteristics, a TEM carbon film is used together with LAO/STO when coating the Pd NPs. Figure 1(b) is an HRTEM image of Pd NPs on a carbon film, where it can be seen that the mean particle size of the Pd NPs is ~2 nm and they are uniformly distributed. (Figure S2 shows the morphology of the Pd NPs on the carbon film at low magnification, and the energy -dispersive X-ray analysis result shows the presence of Pd NPs.) The high-resolution images of the Pd NPs also show clear lattice fringes of Pd, and the inset selected area electron diffraction (SAED) pattern can be indexed as a nanocrystalline fcc structure of Pd.

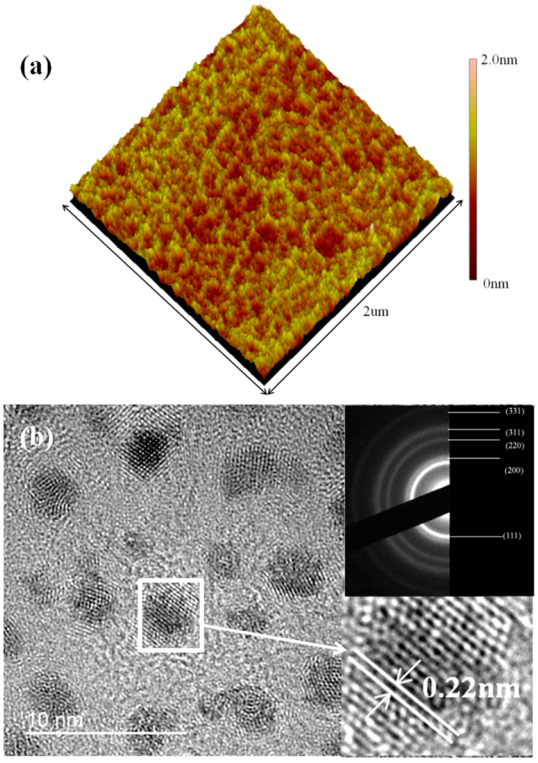

Figure 1. (a) AFM image of Pd NP-modulated LAO surface on STO substrate. (b) HRTEM images showing uniformly distributed Pd NPs with an average size of around 2 nm. The lattice spacings of the particles are indentified to be around 0.22 nm, corresponding to the Pd (111) atomic plane. The inset is a SAED pattern showing the polycrystalline structure of the Pd NPs.

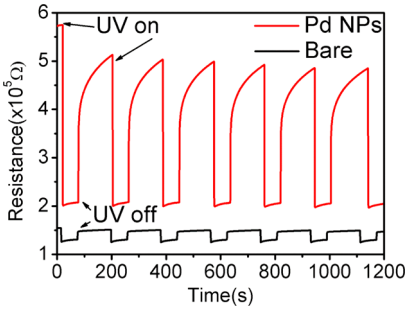

Figure 2. Photoresponse characteristics of the Pd NP-coated LAO/STO (red) and LAO/STO (black) heterostructure showing the reversible switching behavior under periodic illumination of a 365 nm UV light with an incident power density of 10 mW/cm^2.

Photoresponses of the bare (*i.e.*, no Pd NP coating) and Pd NP-coated LAO/STO samples under a repeatable on/off UV light (365 nm) are shown in Figure 2. It can be seen that when the UV light is turned on, both samples change from a high-resistance state to a low-resistance state; when the light is off, the resistance of the interface increases as a function of time. The resistance of the interface decreases within 0.1 s after the UV light is irradiated on both samples, followed by a slow photorecovery process. The increase of resistance of the Pd NP-coated sample in each time interval is much higher than that of the bare

sample. Within 2 min after the light is switched off in each cycle, the resistance is yet to be saturated; this can be attributed to the persistent photoconductivity effect.[17−19] This result reveals that after the surface modification by Pd NPs the LAO/STO interfacial 2DEG is more sensitive to the UV light, making it possible for applications as a UV light sensor.

To understand the mechanism of such a Pd NP-induced enhancement effect, wavelength and time dependences of the photoconductivity for the two samples were characterized. Figure 3 illustrates the wavelength-dependent photoconductivity of the LAO/STO samples (with and without Pd NPs on the surface) at room temperature. The photoconductivity of the heterostructure was measured at 10 V bias, and the samples were irradiated by light with wavelengths ranging from 700 to 300 nm (from low photon energy to high photon energy). The samples were put in the dark environment before measurement, and the measurement started after the resistance reached a stable state. It is noted that, in the dark environment, the resistance of the Pd NP surface modulated LAO/STO heterostructure (∼3 MΩ) is much higher than that of the bare LAO/STO 2DEG, which is ∼0.25 MΩ. The change in photoconductivity is defined by $[(I_{photo} - I_{dark})/I_{dark}] \times 100\%$, where I_{photo} corresponds to the photocurrent under light illumination and I_{dark} corresponds to the dark current. Strong photoconductivity is observed at ∼380 nm, while the increase of photoconductivity for both samples in the wavelength range of 420−700 nm is not obvious. The change in photocurrent for the bare sample at 380 nm is only 18% (a small increase in 420−700 nm is due to the surface trap state), but for the Pd NP-coated LAO/STO sample, the change is 750%, which is a giant photoconductivity. It is worth noting that the 380 nm UV light is around the band gap energy of the STO substrate (3.3 eV), suggesting that the increase of photocurrent is due to the absorption of photon energy by STO and the generation of electron−hole pairs, while the electrons diffuse to the interface as a contribution of the carriers. By contrast, for the photons with energy below the band gap energy, only a very limited number of charge carriers can be generated corresponding to the midgap defect states of the STO substrate from oxygen vacancies during the deposition of the thin film.

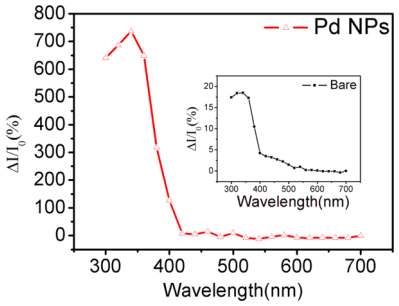

Figure 3. Wavelength-dependent photoresponse, *i.e.*, change of photocurrent (defined as $\Delta I/I_0 = (I_{photo} - I_{dark})/I_{dark}$), for the Pd NP-coated (red) and bare (inset) LAO/STO samples under 10 V bias.

In order to investigate the effect on the photoconductivity in the UV range, the time-dependent resistance of the interface for the bare and Pd NP-coated LAO/STO samples was measured at different ambient conditions (oxygen, dry air, and argon). To circumvent the scattering of the data from sample to sample and rule out the effects of the unwanted experimental factors, the Pd NP-coated LAO/STO heterostructure is prepared from the same piece of sample and the Pd NPs are grown under the same conditions for all measurements. As shown in Figure 4(a), for the recovery process of the LAO/STO sample, the resistance of the 2DEG increases less than 30% in an hour after switching off the UV light in an oxygen and argon environment, suggesting that the change of gas does not affect the transport properties of the interface. However, very different electrical responses for the Pd NP-coated LAO/STO sample under oxygen, dry air, and argon were observed, as shown in Figrue 4(b). With argon gas in the chamber, the resistance of the Pd NP/LAO/STO sample recovers very slowly, having a

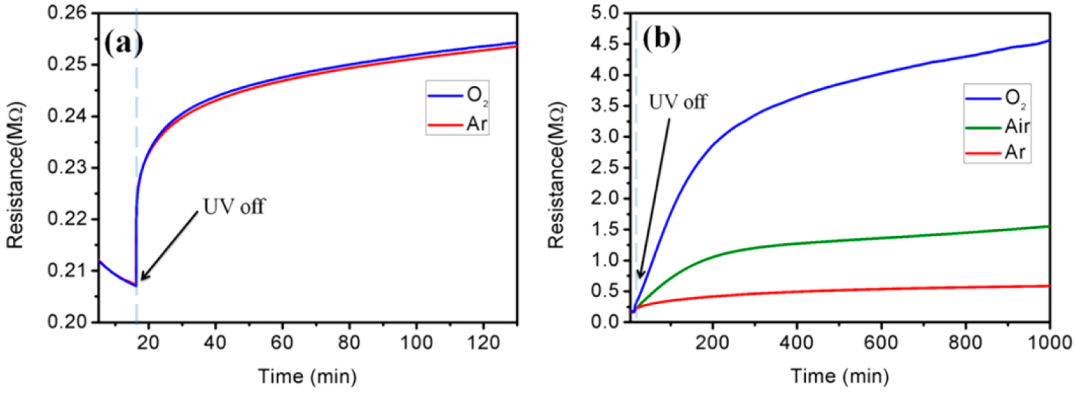

Figure 4. Time-dependent surface resistance under 10 V bias for the (a) bare and (b) Pd NP-coated LAO/STO samples at room temperature.

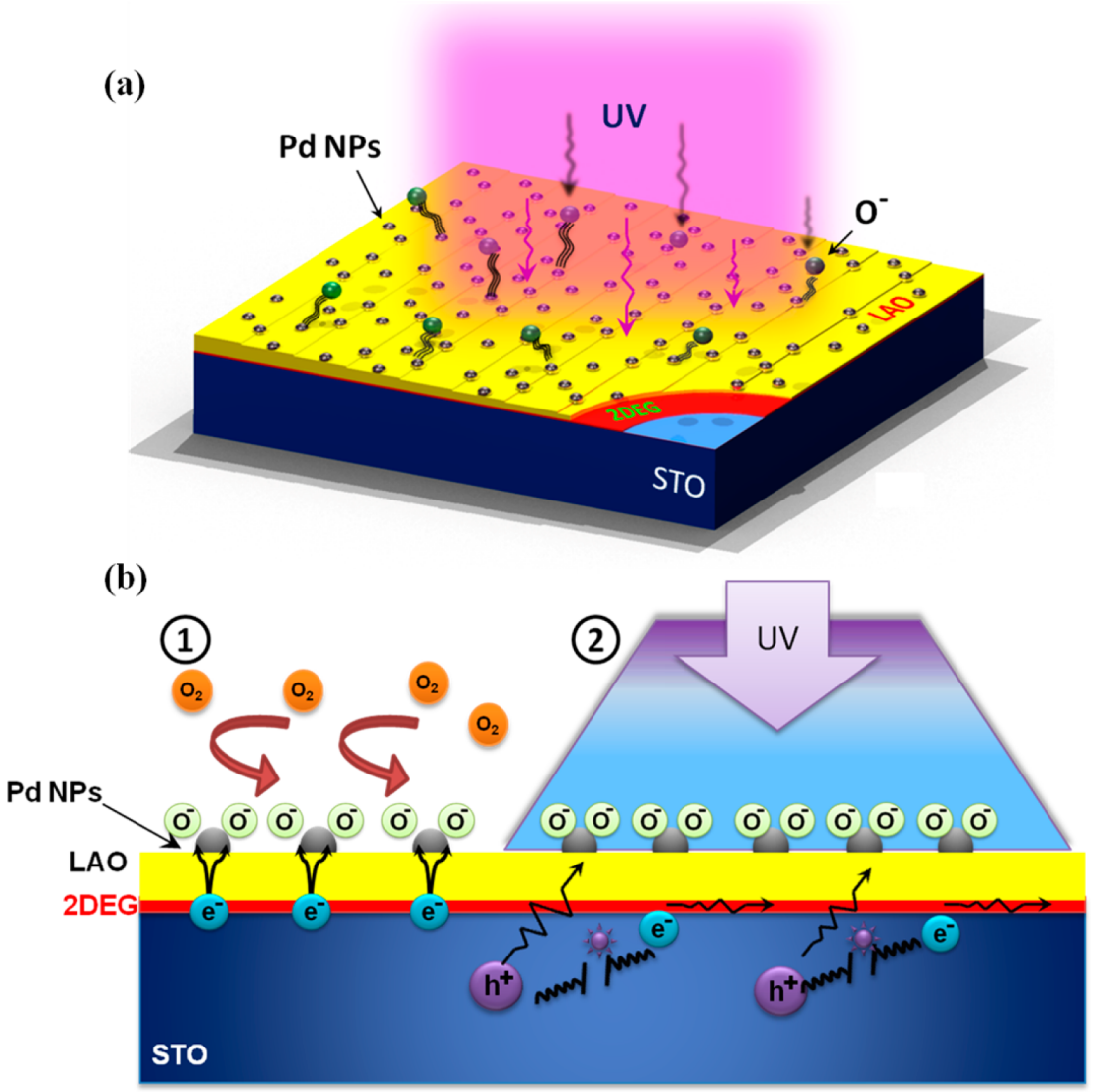

Figure 5. (a) Schematic diagram of the Pd NP surface modulated LAO/STO with UV light irradiation. (b) Schematic depiction of process 1. The oxygen absorbed on Pd NPs attracts electrons from 2DEG, making it negatively charged. In process 2, UV light irradiates the surface and excites electron−hole pairs inside the STO, the photoexcited electrons become excess charge carriers to the 2DEG interface, and photoexcited holes diffuse through LAO and combine with the negatively charged oxygen on the surface of LAO.

similar recovery speed to the case in the bare sample, as shown in Figure 4(a). When the gas ambient is changed from argon to dry air, the speed of the recovery process increases as the result of oxygen adsorption, where Pd NPs are treated as the available surface adsorption sites for oxygen molecules. Futher study shows that recovery of resistance is even faster under pure oxygen gas because more oxygen is available for chemisorption on the Pd NP surface. The photorecovery of the Pd NP-coated LAO/STO heterostructure in different environments can be well fitted by the stretched-expotential law, $I_{photo}(t) = I_{photo}(0) \exp(-t/\tau)\beta$, as shown in Figure S3 (Supporting Information), where τ is the characteristic relaxation time and β is the stretching parameter with values between 0 and 1. Both Figures 3 and 4 show a significant difference of electrical response between the Pd NP-modulated and the bare LAO/STO samples, suggesting enhanced photoconductivity upon UV light illumination; that is, the Pd NPs on LAO/STO significantly enhance the photoconductivity of the interface.

DISCUSSION

To explain this enhanced photoconductivity effect of the Pd NP-coated sample, we propose the following model (as shown in Figure 5). We believe that the presence of Pd NPs and the resulting charge coupling and exchange with the oxygen-deficient LAO film facilitates the interfacial redox reaction at room temperature,[27−30] while from the viewpoint of electronic band structure, the work function of the Pd NP relative to the electron affinity of STO determines the transfer of electrons from the interface to the Pd NPs.

Metals such as Pd with a work function (5.6 eV) larger than the electron affinity of STO (4.0 eV) result in a strong suppression of 2DEG carrier densities at the interface due to the reduction of the internal built-in electric field in the LAO layer; a similar effect has been observed in the recent first-principle calculation.[22,31,32] In addition to this Pd NP electron affinity induced degradation of the 2DEG, the Pd NP's catalytic electrochemical reaction with oxygen molecules is believed to play a more important role in reducing the sheet carrier density (n_s) of the LAO/STO 2DEG. The measured n_s for the bare sample is $\sim 6.5 \times 10^{13}$ cm^{-2} under UV irradiation and $\sim 1.2 \times 10^{13}$ cm^{-2} in the dark, while for the Pd NP-coated LAO/STO, n_s under UV irradiation is measured to be $\sim 3.9 \times 10^{13}$ cm^{-2} and in the dark it is $\sim 3.4 \times 10^{12}$ cm^{-2}. To compare the conducting behavior between the bare LAO/STO and Pd NP-coated LAO/STO sample, the resistance–temperature curves of the samples were measured from room temperature down to 15 K in the "dark" and "under UV irradition" environment, as shown in Figure S4, while UV light with a wavelegnth of 365 nm was irradiated on the sample during cooling. One can see from Figure S4(a,b) that the bare LAO/STO sample shows metallic behavior under UV irradiation and a dark environment. For the Pd NP-coated sample, the interface shows metallic behavior under UV irradiation, as shown in Figure S4(c), while for the Pd NP-coated sample in the dark, as shown in Figure S4(d), the conducting behavior of the interface changed to insulating; that is, the presence of metallic elements on top of LAO may affect the electrical properties of the interface. It is well known that the surface of the Pd NP is very sensitive to the surrounding environment due to the large surface-to-volume ratio, and the Pd NP's surface is usually attached with oxygen molecules when exposed to air.[33,34] The Pd NPs catalytically activate the dissociation of molecular oxygen, and due to the catalytic effect, the interaction between oxygen molecules from the ambient and Pd NPs results in the dissociation of O_2, *i.e.*, $O_2 + 2e^- \rightarrow 2O^-$. A similar phenomenon has been observed in the Pd NP-coated ZnO systems.[24,34] It was proposed that when oxygen molecules from the ambient were absorbed on the exposed surface of Pd NPs, electrons were extracted from the ZnO conduction band, and depletion layers were formed at the surface of ZnO, causing a decrease in carrier concentration. In the LAO/STO system, we believe that oxygen molecules dissociate and generate chemisorbed oxygen species due to the enhanced interaction by Pd NPs on the surface, and the oxygen molecules tend to capture free electrons from the Pd NPs and cause the interfacial 2DEG electrons to diffuse out to the LAO film or the Pd NPs. Therefore, with the absorption of oxygen on the Pd NP surface, O^- tends to "spill over" the surface of the LAO,[25] resulting in more negative charge carriers being trapped on the LAO surface, and therefore, the carrier density of the interfacial 2DEG decreases and the resistance of the interface increases.

On the other hand, when UV light irradiates the surface, more electrons were induced in the 2DEG interface due to the generation of photon-excited electrons and holes in the STO substrate (suggested by the fact that the photocurrent starts to increase when the photon energy exceeds the band gap energy of STO). The persistent increase of the photoresistivity is due to the slow recombination of electrons and holes when the light is off,[17] and the slow recombination process is due to the internal electric field built up from the polar discontinuity in the LAO layer. This field tends to separate electrons and holes (electrons at interface and holes at the surface), and therefore, the recombination is generally prohibited, but the interdiffusion of electrons and holes still results in slow recombination. We conducted electrical measurements on samples with a Pd NP coating on 10 u.c. and 40 u.c. LAO/STO, and the electrical performance of the sample varies with testing condition, as shown in Figure S5, showing slower and smaller photoresponses compared to the sample with the 5 u.c. Pd NP LAO/STO sample. The thicker LAO film hinders the diffusion of electrons to the Pd NPs with increasd diffusion length, so the ratio of resistance recovery is not as high as the case for the 5 u.c. sample

It might be argued that the enhanced photoconductivity could also be due to the surface plasmonic effect, which has been reported in different types of noble metal NPs to improve the catalytic effect in different kinds of systems[35−37] under irradiation of light with a particular wavelength. The high-density electrons in the metal NPs form an electron cloud and oscillate, while the size of the metal particles determines the resonance frequency of the surface plasmon. However, from the previous study, the surface plasmonic resonance effect of small Pd NPs below 10 nm in size should not have significant resonance from 300 to 1500 nm wavelength; therefore the surface plasmonic effect can be ruled out in our case, where the size of Pd NPs is only a few nanometers. We believe that the increased surface-to-volume ratio for Pd NPs and thus the increased catalytic effect of absorbing and dissociation of oxygen molecules in air is responsible for the enhanced photoconductivity.[38] In addition, the change of resistance is an interfacial effect and is not due to the STO substrate,[39] as after irradiation of UV light on the STO substrate the recombination–generation rate of the photoexcited electrons and holes in the substrate is on a nanosecond scale.

The *I*–*V* characteristics of the bare and Pd NP-coated LAO/STO samples were measured under the same conditions. Before the measurement, both samples were put in the dark for 24 h. The *I*–*V* curves for the bare LAO/STO sample in the dark and under UV

light are shown in Figures S6(a), where the ohmic conducting behavior of the interface can be seen and the resistances are found to be 26 kΩ in the dark and 20 kΩ under UV light. The *I*−*V* curve of the bare sample measured under normal room light illumination is almost the same as shown in Figure S6(a), showing less change in resistance. Figure S6(b) shows the *I*−*V* curves for the Pd NP-coated sample measured in the dark, in room light, and under UV irradiation. It is apparent that the *I*−*V* curves exhibit a very large change in slope under different illuminations, indicating a significant change in resistance at the interface.

In summary, the Pd NP modification of the LAO/STO heterostructural surface exhibits oxygen-sensitive, large photoconductivity at room temperature. This interesting phenomenon is attributed to Pd NPs' catalytic effect and surface/interface charge coupling. These results are interesting in physics and can probably be used for sensor applications such as UV light sensing and gas sensing.

EXPERIMENTAL SECTION

A 5 unit cell thick LAO film was deposited on a TiO_2-terminated $SrTiO_3$ (001) substrate with a size of 5 mm × 5 mm by laser-molecular beam epitaxy (laser-MBE) using a KrF excimer laser (Lambda Physik COMPex 205, wavelength = 248 nm) at 1 Hz and a single-crystalline $LaAlO_3$ target. During deposition, the substrate temperature was maintained at 750 °C with a base vacuum lower than 2×10^{-5} Pa; the growth was monitored by reflection high-energy electron diffraction (RHEED). After deposition, the samples were *in situ* annealed at a reduced temperature of 550 °C at 1000 Pa O_2 for 1 h, in order to reduce oxygen vacancies in the film. The sample was then cooled to room temperature in the same ambient. After the deposition, Hall and sheet resistance measurements were carried out to characterize the 2DEG nature of the interface. Palladium NPs were deposited on the LAO/STO surface using dc magnetron sputtering at room temperature under a power of 15 W with Ar gas (99.995%) having a flow rate of 10 sccm at a pressure of 100 mTorr. The deposition time was optimized to make sure that the Pd NPs did not form a complete conducting path on the LAO/STO surface. A TEM grid with a carbon film was put close to the sample during the deposition of palladium for subsequent TEM structural analysis (since it is room-temperature growth, the Pd NPs on the carbon film can roughly represent the structure of the Pd NPs on the LAO surface). High-resolution TEM (HRTEM, JEOL 3000FX operating at 300 kV) was used for the nanoparticle analysis. The samples were ultrasonically wire-bound with Al wires, and the two-probe electrical characteristics were measured by an electrometer under a dc bias of 10 V in a stainless steel vacuum chamber with oxygen, dry air, and argon, respectively, both with 99.9995% purity. A UV light source was induced into the chamber for photoresistance measurement. Light of different wavelengths was generated with a standard system equipped with a monochromator (Newport 66902) and a dual-channel power meter (Newport 2931-C).

Conflict of Interest: The authors declare no competing financial interest.

Supporting Information Available: Figures S1−S6. This material is available free of charge *via* the Internet at http://pubs.acs.org.

Acknowledgment. N.Y.C. would like to thank the Hong Kong Ph.D. Fellow Scheme from the Research Grants Council of Hong Kong No. RUY3 for support. This work was supported by the National Key Basic Research Program of China (973 Program) under Grant No. 2013CB632900, GRF Grant No.514512, and the PolyU internal grant No. G-YJ169.

REFERENCES AND NOTES

1. Hwang, H. Y.; Iwasa, Y.; Kawasaki, M.; Keimer, B.; Nagaosa, N.; Tokura, Y. Emergent Phenomena at Oxide Interfaces. *Nat. Mater.* **2012**, *11*, 103–113.
2. Ohtomo, A.; Hwang, H. Y. A High-Mobility Electron Gas at the $LaAlO_3/SrTiO_3$ Heterointerface. *Nature* **2004**, *427*, 423–426.
3. Thiel, S.; Hammerl, G.; Schmehl, A.; Schneider, C. W.; Mannhart, J. Tunable Quasi-Two-Dimensional Electron Gases in Oxide Heterostructures. *Science* **2006**, *313*, 1942–1945.
4. Pauli, S.; Leake, S.; Delley, B.; Björck, M.; Schneider, C.; Schlepütz, C.; Martoccia, D.; Paetel, S.; Mannhart, J.; Willmott, P. Evolution of the Interfacial Structure of $LaAlO_3$ on $SrTiO_3$. *Phys. Rev. Lett.* **2011**, *106*, 036101.
5. Singh-Bhalla, G.; Bell, C.; Ravichandran, J.; Siemons, W.; Hikita, Y.; Salahuddin, S.; Hebard, A. F.; Hwang, H. Y.; Ramesh, R. Built-in and Induced Polarization across $LaAlO_3/SrTiO_3$ Heterojunctions. *Nat. Phys.* **2010**, *7*, 80–86.
6. Cen, C.; Thiel, S.; Mannhart, J.; Levy, J. Oxide Nanoelectronics on Demand. *Science* **2009**, *323*, 1026–1030.
7. Forg, B.; Richter, C.; Mannhart, J. Field-Effect Devices Utilizing $LaAlO_3$-$SrTiO_3$ Interfaces. *Appl. Phys. Lett.* **2012**, *100*, 053506.
8. Bark, C. W.; Sharma, P.; Wang, Y.; Baek, S. H.; Lee, S.; Ryu, S.; Folkman, C. M.; Paudel, T. R.; Kumar, A.; Kalinin, S. V; *et al.* Switchable Induced Polarization in $LaAlO_3/SrTiO_3$ Heterostructures. *Nano Lett.* **2012**, *12*, 1765–1771.
9. Segal, Y.; Ngai, J. H.; Reiner, J. W.; Walker, F. J.; Ahn, C. H. X-ray Photoemission Studies of the Metal-Insulator Transition in $LaAlO_3/SrTiO_3$ Structures Grown by Molecular Beam Epitaxy. *Phys. Rev. B: Condens. Matter Mater. Phys.* **2009**, *80*, 241107.
10. Slooten, E.; Zhong, Z.; Molegraaf, H. J. a.; Eerkes, P. D.; de Jong, S.; Massee, F.; van Heumen, E.; Kruize, M. K.; Wenderich, S.; Kleibeuker, J. E.; *et al.* Hard X-ray Photoemission and Density Functional Theory Study of the Internal Electric Field in $SrTiO_3/LaAlO_3$ Oxide Heterostructures. *Phys. Rev. B: Condens. Matter Mater. Phys.* **2013**, *87*, 085128.
11. Willmott, P.; Pauli, S.; Herger, R.; Schlepütz, C.; Martoccia, D.; Patterson, B.; Delley, B.; Clarke, R.; Kumah, D.; Cionca, C.; *et al.* Structural Basis for the Conducting Interface between $LaAlO_3$ and $SrTiO_3$. *Phys. Rev. Lett.* **2007**, *99*, 155502.
12. Qiao, L.; Droubay, T. C.; Shutthanandan, V.; Zhu, Z.; Sushko, P. V; Chambers, S. Thermodynamic Instability at the Stoichiometric $LaAlO_3/SrTiO_3$(001) Interface. *J. Phys.: Condens. Matter* **2010**, *22*, 312201.
13. Siemons, W.; Koster, G.; Yamamoto, H.; Harrison, W.; Lucovsky, G.; Geballe, T.; Blank, D.; Beasley, M. Origin of Charge Density at $LaAlO_3$ on $SrTiO_3$ Heterointerfaces: Possibility of Intrinsic Doping. *Phys. Rev. Lett.* **2007**, *98*, 196802.
14. Kalabukhov, A.; Gunnarsson, R.; Börjesson, J.; Olsson, E.; Claeson, T.; Winkler, D. Effect of Oxygen Vacancies in the $SrTiO_3$ Substrate on the Electrical Properties of the $LaAlO_3/SrTiO_3$ Interface. *Phys. Rev. B: Condens. Matter Mater. Phys.* **2007**, *75*, 121404(R).
15. Xie, Y.; Hikita, Y.; Bell, C.; Hwang, H. Y. Control of Electronic Conduction at an Oxide Heterointerface Using Surface Polar Adsorbates. *Nat. Commun.* **2011**, *2*, 494.
16. Au, K.; Li, D. F.; Chan, N. Y.; Dai, J. Y. Polar Liquid Molecule Induced Transport Property Modulation at $LaAlO_3/SrTiO_3$ Heterointerface. *Adv. Mater.* **2012**, *24*, 2598–2602.
17. Rastogi, A.; Budhani, R. C. Solar Blind Photoconductivity in Three-Terminal Devices of $LaAlO_3/SrTiO_3$ Heterostructures. *Opt. Lett.* **2012**, *37*, 317–319.

18. Tebano, A.; Fabbri, E.; Pergolesi, D.; Balestrino, G.; Traversa, E. Room-Temperature Giant Persistent Photoconductivity in $SrTiO_3/LaAlO_3$ Heterostructures. *ACS Nano* **2012**, *6*, 1278–1283.
19. Scotti, U.; Aruta, C.; Cantoni, C.; Di Gennaro, E.; Lupini, A. R.; Maccariello, D.; Marré, D.; Pallecchi, I.; Paparo, D.; Perna, P.; Riza, M.; Granozio. F. Reversible and Persistent Photoconductivity at the $NdGaO_3/SrTiO_3$ Conducting Interface. arXiv:1206.5083v1.
20. Rastogi, A.; Kushwaha, A. K.; Shiyani, T.; Gangawar, A.; Budhani, R. C. Electrically Tunable Optical Switching of a Mott Insulator-Band Insulator Interface. *Adv. Mater.* **2010**, *22*, 4448–4451.
21. Irvin, P.; Ma, Y.; Bogorin, D. F.; Cen, C.; Bark, C. W.; Folkman, C. M.; Eom, C.; Levy, J. Rewritable Nanoscale Oxide Photodetector. *Nat. Photonics* **2010**, *4*, 849–852.
22. Arras, R.; Ruiz, V.; Pickett, W.; Pentcheva, R. Tuning the Two-Dimensional Electron Gas at the $LaAlO_3/SrTiO_3$ (001) Interface by Metallic Contacts. *Phys. Rev. B: Condens. Matter Mater. Phys.* **2012**, *85*, 125404.
23. Bristowe, N.; Littlewood, P.; Artacho, E. Surface Defects and Conduction in Polar Oxide Heterostructures. *Phys. Rev. B: Condens. Matter Mater. Phys.* **2011**, *83*, 205405.
24. Chang, Y.; Xu, J.; Zhang, Y.; Ma, S.; Xin, L.; Zhu, L.; Xu, C. Optical Properties and Photocatalytic Performances of Pd Modified ZnO Samples. *J. Phys. Chem. C* **2009**, *113*, 18761–18767.
25. Kolmakov, A.; Klenov, D. O.; Lilach, Y.; Stemmer, S.; Moskovits, M. Enhanced Gas Sensing by Individual SnO_2 Nanowires and Nanobelts Functionalized with Pd Catalyst Particles. *Nano Lett.* **2005**, *5*, 667–673.
26. Ye, M.; Gong, J.; Lai, Y.; Lin, C.; Lin, Z. High-Efficiency Photoelectrocatalytic Hydrogen Generation Enabled by Palladium Quantum Dots-Sensitized TiO_2 Nanotube Arrays. *J. Am. Chem. Soc.* **2012**, *134*, 15720–15723.
27. Lee, S. W.; Liu, Y.; Heo, J.; Gordon, R. G. Creation and Control of Two-Dimensional Electron Gas Using Al-Based Amorphous Oxides/$SrTiO_3$ Heterostructures Grown by Atomic Layer Deposition. *Nano Lett.* **2012**, *12*, 4775–4783.
28. Liu, Z. Q.; Li, C. J.; Lü, W. M.; Huang, X. H.; Huang, Z.; Zeng, S. W.; Qiu, X. P.; Huang, L. S.; Annadi, A.; Chen, J. S.; *et al*. Origin of the Two-Dimensional Electron Gas at $LaAlO_3$/$SrTiO_3$ Interfaces: The Role of Oxygen Vacancies and Electronic Reconstruction. *Phys. Rev. X* **2013**, *3*, 021010.
29. Trier, F.; Christensen, D. V.; Chen, Y. Z.; Smith, A.; Andersen, M. I.; Pryds, N. Degradation of the Interfacial Conductivity in $LaAlO_3/SrTiO_3$ Heterostructures during Storage at Controlled Environments. *Solid State Ionics* **2013**, *230*, 12–15.
30. Chen, Y.; Pryds, N.; Kleibeuker, J. E.; Koster, G.; Sun, J.; Stamate, E.; Shen, B.; Rijnders, G.; Linderoth, S. Metallic and Insulating Interfaces of Amorphous $SrTiO_3$-Based Oxide Heterostructures. *Nano Lett.* **2011**, *11*, 3774–3778.
31. Janotti, A.; Bjaalie, L.; Gordon, L.; Van de Walle, C. G. Controlling the Density of the Two-Dimensional Electron Gas at the $SrTiO_3/LaAlO_3$ Interface. *Phys. Rev. B: Condens. Matter Mater. Phys.* **2012**, *86*, 241108.
32. Lee, J.; Lin, C.; Demkov, A. A. Metal-Induced Charge Transfer, Structural Distortion, and Orbital Order in $SrTiO_3$ Thin Films. *Phys. Rev. B: Condens. Matter Mater. Phys.* **2013**, *87*, 165103.
33. Meusel, I.; Hoffmann, J.; Hartmann, J. The Interaction of Oxygen with Alumina-Supported Palladium Particles. *Catal. Lett.* **2001**, *71*, 5–13.
34. Bera, A.; Basak, D. Pd-Nanoparticle-Decorated ZnO Nanowires: Ultraviolet Photosensitivity and Photoluminescence Properties. *Nanotechnology* **2011**, *22*, 265501.
35. Chen, T.; Xing, G. Z.; Zhang, Z.; Chen, H. Y.; Wu, T. Tailoring the Photoluminescence of ZnO Nanowires Using Au Nanoparticles. *Nanotechnology* **2008**, *19*, 435711.
36. Teranishi, T.; Eguchi, M.; Kanehara, M.; Gwo, S. Controlled Localized Surface Plasmon Resonance Wavelength for Conductive Nanoparticles over the Ultraviolet to Near-Infrared Region. *J. Mater. Chem.* **2011**, *21*, 10238.
37. Huang, X.; Tang, S.; Mu, X.; Dai, Y.; Chen, G.; Zhou, Z.; Ruan, F.; Yang, Z.; Zheng, N. Freestanding Palladium Nanosheets with Plasmonic and Catalytic Properties. *Nat. Nanotechnol.* **2011**, *6*, 28–32.
38. Xiong, Y.; Chen, J.; Wiley, B.; Xia, Y.; Yin, Y.; Li, Z.-Y. Size-Dependence of Surface Plasmon Resonance and Oxidation for Pd Nanocubes Synthesized *via* a Seed Etching Process. *Nano Lett.* **2005**, *5*, 1237–1242.
39. Rubano, A.; Paparo, D.; Miletto, F.; Scotti di Uccio, U.; Marrucci, L. Recombination Kinetics of a Dense Electron-Hole Plasma in Strontium Titanate. *Phys. Rev. B: Condens. Matter Mater. Phys.* **2007**, *76*, 125115.